SAND2014-4739C

Diagnostics of radiation source geometric dilution with parallax for iron opacity experiments

T. Nagayama,[1] J.E. Bailey,[1] S.B. Hansen,[1] G. Loisel,[1] and G.A. Rochau[1]
Sandia National Laboratories, Albuquerque, New Mexco 87185, USA

(Dated: 27 May 2014)

Experimental tests are in progress to evaluate the accuracy of the modeled iron opacity at solar interior conditions [J.E. Bailey et al., Phys. Plasmas 16, 058101 (2009)]. The iron sample is placed on top of the Sandia National Laboratories z-pinch dynamic hohlraum (ZPDH) radiation source. The samples are heated to 150 - 200 eV electron temperatures and 7×10^{21} - 4×10^{22} cm^{-3} electron densities by the ZPDH radiation and backlit at its stagnation [T. Nagayama et al., Phys. Plasmas 21, 056502 (2014)]. The backlighter attenuated by the heated sample plasma is measured by four spectrometers along 0 and/or ± 9° with respect to the z-pinch axis to infer the sample iron opacity. Here we describe measurements of the source-to-sample distance that exploit the parallax of spectrometers that view the half-moon-shaped sample from ± 9° with respect to the z-pinch axis. We observe that the measured sample temperature decreases with increased source to sample distance, implying that this distance must be taken into account for understanding the sample heating.

I. INTRODUCTION

Opacity quantifies photon absorption in matter and plays a crucial role in many high energy density (HED) plasmas, including inertial fusion plasmas and stellar interiors[1]. As temperature and density increase, modeling opacity becomes more challenging and employs approximations that need to be experimentally validated[2,3]. Performing reliable opacity experiments is also challenging and has to satisfy many criteria[2,3]. Measuring opacity becomes more challenging at higher temperature because the opacity sample has to be heated to the high temperature without significant gradients and has to be backlit by a bright radiation to minimize the effect of the hot sample plasma emission on the absorption measurement. Sandia National Laboratories (SNL) Z machine (Z) provides a unique platform to perform opacity experiments at temperatures above 150 eV[4].

The Z-pinch dynamic hohlraum (ZPDH) is a terawatt x-ray radiation source at Z that makes high-temperature opacity measurements possible[5]. The opacity sample is located above the ZPDH radiation source and is radiatively heated. Most of the photons have energies above 600 eV. This powerful radiation streams through the sample and heats it to a target temperature without significant gradients[6]. The ZPDH also provides a bright backlighter to mitigate the sample self-emission. Recently, we found that the opacity sample can reach higher temperatures and densities using the same radiation source only by changing the target configuration[6,7]. However, it was not clear why the change in the target configuration affects the sample temperature if the sample is radiatively by the same radiation source. To make the best use of this high temperature opacity experimental platform, it is crucial to understand what determines the sample temperature. In this article, we provide experimental evidence using parallax to this end.

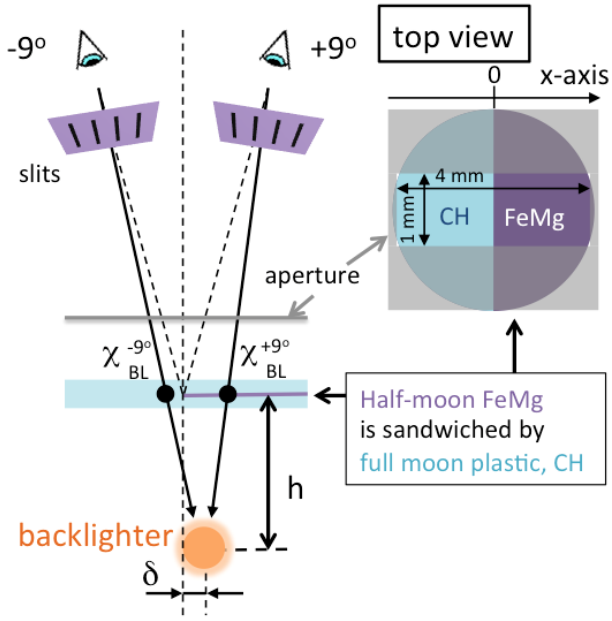

FIG. 1. (Color online) Two spectrometers located at ±9°with respect to the z-axis record the sample transmitted backlighter images. Due to the angle difference, the spectrometers at ±9° see the backlighter centered at different locations on the sample (i.e., $x_{BL}^{+9^\circ}$ and $x_{BL}^{-9^\circ}$). This parallax helps not only to measure FeMg attenuated and unattenuated spectra simultaneously, but also to characterize the backlighter relative location with respect to the "half-moon" boundary, h and δ.

II. SNL OPACITY EXPERIMENTS AND PARALLAX

The typical SNL opacity experimental setup is shown in Fig. 1. The target consists of a semi-circular FeMg sample sandwiched by a circular tamping material (e.g., plastic, CH), which we call a "half-moon" target. Mg is mixed in the Fe sample to diagnose the Fe conditions (i.e., electron temperature, T_e, and electron density, n_e)

with Mg K-shell spectroscopy[6,8]. This target is placed on the top of the ZPDH radiation source, and the ZPDH radiation heats and backlights the sample[3,5]. The backlighter attenuated through the target is recorded by KAP crystal spectrometers fielded along ±9° from the z-axis. An aperture on the top of the target limits the spectrometers' views to a 4 mm × 1 mm area. Each spectrometer has 4∼6 slits, each 50 μm in width, at the halfway distance to the sample to provide spatial resolution of ∼0.1 mm along the aperture direction with a magnification of ∼1. The transmitted backlighter images are recorded on Kodak 2492 x-ray films with spatial and spectral resolution.

Due to the finite source-to-sample distance, h, the spectrometer at +9° would observe the backlighter bright spot through the FeMg embedded side at $x_{BL}^{+9^\circ}$, while the one at −9° would observe it on the CH-only side at $x_{BL}^{-9^\circ}$ (black dots in Fig. 1). The original motivation of this spectrometer configuration is to measure FeMg attenuated and unattenuated spectra simultaneously, then infer FeMg transmission spectra in a single experiment. However, taking advantage of this parallax, we can also infer the backlighter location with respect to the half-moon boundary (i.e., h and δ in Fig. 1) based on $x_{BL}^{+9^\circ}$ and $x_{BL}^{-9^\circ}$ as follows:

$$h = \frac{x_{BL}^{+9^\circ} - x_{BL}^{-9^\circ}}{2\tan(9^\circ)} \quad (1)$$

$$d = \frac{1}{2}\left(x_{BL}^{+9^\circ} + x_{BL}^{-9^\circ}\right) \quad (2)$$

assuming that the source-to-detector distance is much longer than the apparent backlighter peak separations, $x_{BL}^{+9^\circ}$ - $x_{BL}^{-9^\circ}$.

To extract $x_{BL}^{+9^\circ}$ and $x_{BL}^{-9^\circ}$ from the data, one has to understand what difference is expected from the emergent intensity spatial profiles measured at ±9°. Figure 2 shows a schematic of how the emergent intensity spatial profiles would look at ±9°. The x-axis is defined such that the "half-moon" boundary is at x=0 and the FeMg-embedded region is at x>0. The transmission spatial profile (blue) is systematically lower at x>0 due to extra attenuation by FeMg. The backlighter spatial profiles (green) would center at different locations on the sample for the ±9° spectrometers (i.e., $x_{BL}^{+9^\circ}$ and $x_{BL}^{-9^\circ}$, respectively). While most of the backlighter is attenuated through the FeMg region to the spectrometer at +9°, only the backlighter wing is attenuated through FeMg to the spectrometer at −9°. As a result, one expects to see a double-peak in the emergent spatial profile at +9°, while one expect to see a skewed single peak at −9°.

Figure 3 shows actual data recorded by the spectrometers at ±9°. Each image is the average over four slit images to improve the signal-to-noise ratio and to average out random issues across the individual slit images[6]. The horizontal (spectral) and vertical (spatial) axes are

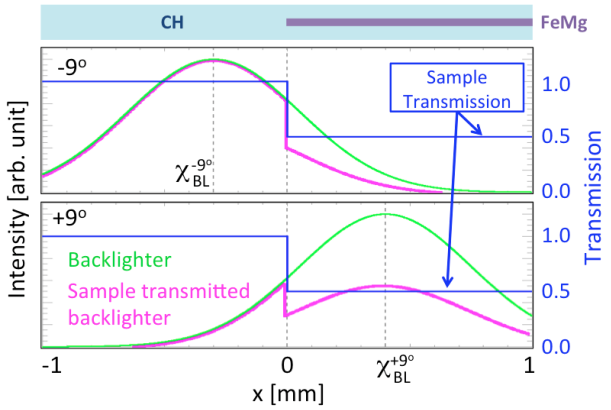

FIG. 2. (Color online) Schematics to illustrate how the backlighter (green) transmitting through different point on the sample would result in different emergent intensity spatial profiles (magenta).

produced by the KAP crystals and the slits, respectively. The dark vertical lines correspond to Fe or Mg bound-bound absorption lines, and it is evident that the image recorded at +9° shows longer Fe and Mg lines than those recorded at −9° because of the apparent backlighter peak location (Fig. 2).

In order to define $x_{BL}^{+9^\circ}$ and $x_{BL}^{-9^\circ}$ for the parallax, one has to extract the locations of the "half-moon" boundary and the apparent backlighter peak. To objectively extract them, we select a strong bound-bound absorption line and take its spatial lineout. The magenta curves in Fig. 4 show an example for Mg Heα line (i.e., absorption due to $1s^2 - 1s2p$ transition by He-like Mg) at around 9.17Å ($\Delta\lambda$=0.02 Å). As discussed earlier, the magenta curve at +9° has a double peak, while the one at −9° has a skewed single peak. If we have similar spatial profiles but without Mg Heα absorption, we could extract the Mg Heα bound-bound line transmission spatial profile and define where the Mg-embedded region starts (i.e., the "half-moon" boundary or x=0). We can approximate such profiles by averaging the two spatial lineouts taken at both sides of Mg Heα line (green in Fig. 4). Their lineout locations for the +9° image are indicated by green dashed lines in Fig. 3. The resultant transmission spatial profiles clearly show low-transmission FeMg embedded regions, and the x-axis is defined from its inflection point. We note that the half-moon boundary is not as sharp as the one in Fig. 2. This is because of the spatial resolution of the instrument and the sample hydrodynamics integrated over the backlighter duration. Once $x_{BL}^{+9^\circ}$ and $x_{BL}^{-9^\circ}$ are defined by the apparent backlighter peak locations on the defined x-axis, the backlighter location, h and δ, can be estimated from Eq. 1 and 2, respectively.

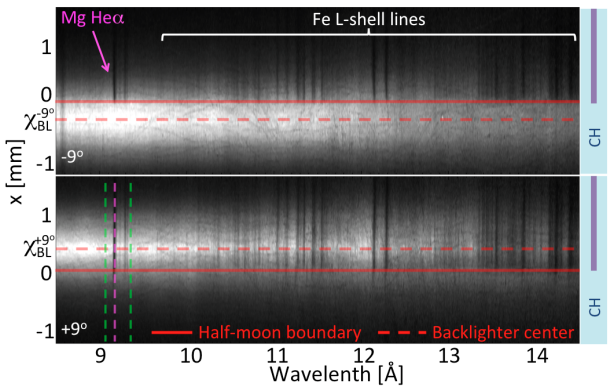

FIG. 3. (Color online) Backlighter images attenuated through the target recorded from -9° (top) and $+9^\circ$ (bottom). FeMg are embedded where x>0. Red solid and dashed lines indicate the locations of the "half-moon" boundary at x=0 and the apparent backlighter peaks at x=$x_{BL}^{-9^\circ}$ and x=$x_{BL}^{+9^\circ}$, respectively.

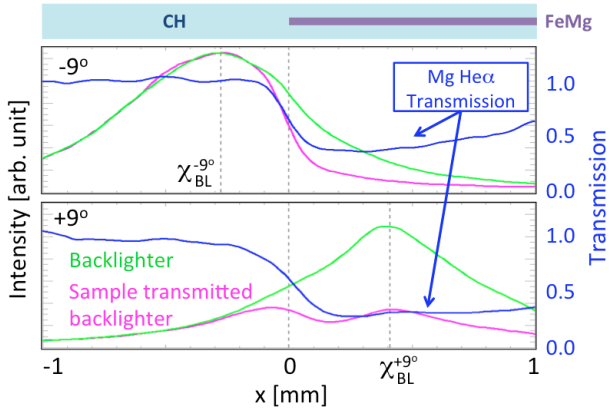

FIG. 4. (Color online) Spatial lineouts are extracted from FIG. 3 at Mg Heα (magenta) and its nearby continuum (green). Mg Heα bound-bound line transmission spatial lineouts (blue) are extracted by dividing the Mg Heα lineouts by the continuum lineouts. The half-moon boundary and the x-axis are defined based on the transmission spatial lineouts, and $x_{BL}^{-9^\circ}$ and $x_{BL}^{+9^\circ}$ are defined based on the continuum peaks.

III. RESULTS

Parallax is systematically applied to ten Fe opacity experiments performed under different CH configurations[6]. There are three different CH configurations and multiple different Fe thicknesses for each configuration. There is one experiment where the sample is raised by 1.5 mm from its nominal location. For each shot, parallax is applied to available bound-bound lines, and the mean h and its uncertainty are inferred by taking the average and the standard deviation over the parallax results from the different lines. Figure 5 summarizes the measured h as a function of Fe T_e inferred from Mg K-shell spectroscopy[6]. We confirm a strong anti-correlation (correlation $\sim$ -0.87) between h and the Fe T_e. A linear fit to the data indicates that the Fe T_e would drop by 36 eV as h is increased by 1 mm.

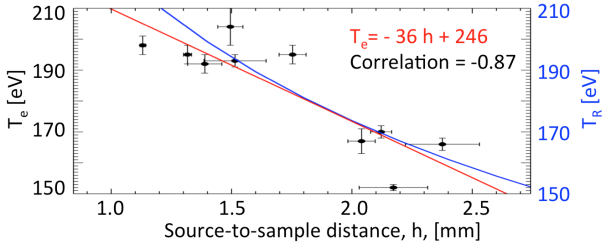

FIG. 5. (Color online) Measured electron temperature, T_e, as a function of the measured source-to-sample distances, h. There is a correlation between sample temperatures and h. The red line is the linear fit to the data, and the blue curve is a modeled heating radiation temperature as a function of h.

To investigate this point synthetically, we use a 3D view factor code VISRAD [Ref] and a calibrated ZPDH intensity image from one of our experiments to calculate the radiation temperature at the sample as a function of the sample distance from the ZPDH radiation source. The details of the calculation will be discussed elsewhere. The resultant heating irradiance can be converted to the temperature that the sample would reach by $T_R = \left(I^{VISRAD}/2\sigma\right)^{1/4}$ where σ is the Stefan-Boltzmann constant. The result is shown in blue in Fig. 5. This explains why the same radiation source heats the sample to different temperatures, and our measurements provide the evidence of this source radiation geometric dilution.

The sample source distance would be determined by three factors: i) initial sample location, ii) radiation source location with respect to the initial sample location, and iii) the hydrodynamics of the sample. The reproducibility of the Fe sample condition is experimentally confirmed[6]. Thus, for the target configurations fielded in the past, we may be able to control the sample temperature by adjusting the sample initial locations.

ACKNOWLEDGMENTS

We thank R. Falcon for his help on refining the paper. Sandia is a multiprogram laboratory operated by Sandia Corporation, a Lockheed Martin Company, for the (U.S.) Department of Energy under Contract No. DE-AC04-94AL85000.

[1]D. Mihalas, *Stellar Atmospheres*, A Series of books in astronomy and astrophysics (W. H. Freeman, 1978).
[2]T. Perry *et al.*, Phys. Rev. E **54**, 5617 (1996).
[3]J. E. Bailey *et al.*, Physics of Plasmas **16**, 058101 (2009).
[4]J. Bailey *et al.*, Physical Review Letters **99** (2007).
[5]G. A. Rochau *et al.*, Physics of Plasmas (1994-present) **21**, 056308 (2014).
[6]T. Nagayama *et al.*, Physics of Plasmas (1994-present) **21**, 056502 (2014).
[7]T. J. Nash *et al.*, Rev. Sci. Instrum. **81**, 10E518 (2010).
[8]J. E. Bailey *et al.*, Rev. Sci. Instrum. **79**, 113104 (2008).